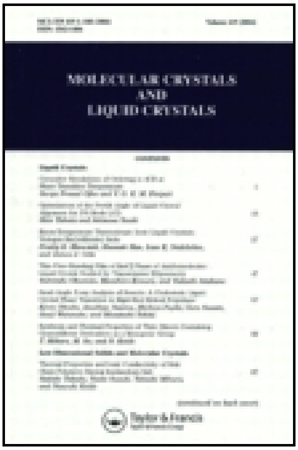

Molecular Crystals and Liquid Crystals
Publication details, including instructions for authors and subscription information:
http://www.tandfonline.com/loi/gmcl20

Phase Transitions and Physical Properties of a Binary Mixture of Bicyclohexane Compounds, I: Refractive Index Measurements

Prithwi Dev Roy [a], Malay Kumar Das [a], Sukla Paul [a], Ranjit Paul [a] & Banani Das [b]

[a] Department of Physics, North Bengal University, Siliguri, India

[b] Department of Physics, Siliguri Institute of Technology, Siliguri, India

Version of record first published: 31 Jan 2007

To cite this article: Prithwi Dev Roy, Malay Kumar Das, Sukla Paul, Ranjit Paul & Banani Das (2006): Phase Transitions and Physical Properties of a Binary Mixture of Bicyclohexane Compounds, I: Refractive Index Measurements, Molecular Crystals and Liquid Crystals, 457:1, 43-53

To link to this article: http://dx.doi.org/10.1080/15421400500447124

Mol. Cryst. Liq. Cryst., Vol. 457, pp. 43–53, 2006
Copyright © Taylor & Francis Group, LLC
ISSN: 1542-1406 print/1563-5287 online
DOI: 10.1080/15421400500447124

Phase Transitions and Physical Properties of a Binary Mixture of Bicyclohexane Compounds, I: Refractive Index Measurements

Prithwi Dev Roy
Malay Kumar Das
Sukla Paul
Ranjit Paul
Department of Physics, North Bengal University, Siliguri, India

Banani Das
Department of Physics, Siliguri Institute of Technology, Siliguri, India

Binary mixtures of two alkenyl side chain bicyclohexane compounds have been prepared, one a pure nematic phase (1d(3)CCO$_2$) and the other a pure smectic B phase (0d(4)CCO$_2$). These two compounds are characterized by similar molecular structure, except for a shift in the position of the double bond. An interesting observation in the phase diagram is the occurrence of a two-phase (smectic B–nematic) co-existing region (≈2.5–3°C) for a small concentration range ($x = 0.55$–0.8) for these mixtures. Density and refractive indices (n_o, n_e) have been measured for these mixtures. In the co-existing smectic B–nematic phase, we have been able to measure simultaneously the refractive indices of both the smectic B and the nematic phases. The refractive index and density values have been analyzed to yield orientational order parameters. From the Differential Scanning Calorimetry (DSC), density, and birefringence measurements, the nature of the smectic B–nematic phase transition for these mixtures has been assessed. The behavior of this phase transition with concentration is also reported.

Keywords: density; orientational order parameter; refractive index

INTRODUCTION

Liquid-crystalline material research has contributed significantly both to the development of liquid-crystalline display (LCD) technology and also to the better understanding of the phase behavior of soft

Address correspondence to Malay Kumar Das, Department of Physics, North Bengal University, Siliguri 734430, India. E-mail: mkdnbu@yahoo.com

condensed matter systems. Quantitative knowledge of orientational ordering is necessary so that improved materials may be devised for applications. Thus, attempts are continuously being made to study the material properties of both pure compounds as well as their mixtures for a better insight into the basic understanding of liquid-crystalline behavior so that a newer and more acceptable class of materials suitable for display devices emerges.

In this work, we present the phase diagram, birefringence, DSC, and density measurements of a binary mixture of two nonpolar bicyclohexane compounds containing alkenyl side chains. So far, there are only a few liquid-crystalline classes described in the literature whose rigid core consists of two cyclohexane rings. The physical properties of the pure components have been studied previously in our laboratory [1–4]. These two compounds, one of only nematic–phase (1d(3)CCO_2) and the other of only smectic B (SmB) phase (0d(4)CCO_2), are characterized by a similar molecular structure, except for a shift in the position of the double bond. Schadt *et al.* [5] showed that the introduction of a double bond at specific side-chain positions markedly affects the physical properties of liquid crystals. To study the effect of the position of double bond in the alkenyl side chain on the mesomorphic properties, mixtures of these compounds have been prepared. Physical properties of these mixtures have been studied at seven different compositions. A phase diagram for this system shows the presence of mixtures with only SmB phase, only N phase, and both SmB and N phases. A two-phase (SmB-N) co-existing region ($\sim$2–3°C) has also been observed for a small concentration range for these mixtures. DSC studies of these mixtures have been done, and the entropy changes associated with the SmB-N and N-isotropic (I) phase transition have been calculated. Densities and refractive indices (n_o, n_e) have been measured for these mixtures. The refractive index data have been analyzed to yield orientational order parameters. From the DSC, density, and birefringence measurements, the nature of the SmB-N phase transition for these mixtures and the behavior of these phase transitions with concentration has been assessed.

EXPERIMENTAL

Phase Diagram and Texture Study

The compounds were donated to us by M/S Hoffmann-La-Roche and Co., Basel, Switzerland, and were used without further purification. Phase transitions of the pure samples as well as their mixtures were studied by observing textures under crossed polarizers with a polarizing microscope equipped with a Mettler FP80/82 thermosystem.

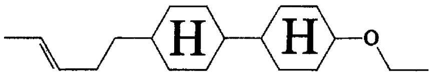

SCHEME 1 Component 1: $C \underset{24.5^\circ C}{\overset{44^\circ C}{\rightleftharpoons}} N \xrightarrow{76.5^\circ C} I$. 4(3″-Pentenyl) 4′(ethoxyl) 1,1′ bicyclohexane (ld(3)CCO_2).

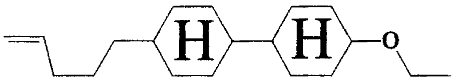

SCHEME 2 Component 2: $C \xrightarrow{11^\circ C} Sm\ B \xrightarrow{43^\circ C} I$. 4-Ethoxy, 4′-pent-4″-enyl bicyclohexane (0d(4)CCO_2).

The structural formula, transition temperatures, and chemical name of the pure compounds are shown in Schemes 1 and 2.

The phase diagram of this system as observed by us is shown in Fig. 1. The N-I and SmB-N transition temperatures are plotted against molar fraction (x) of ld(3)CCO_2 in Fig. 1. Also plotted on the same figure are the melting temperatures. Due to lack of cooling facilities in our

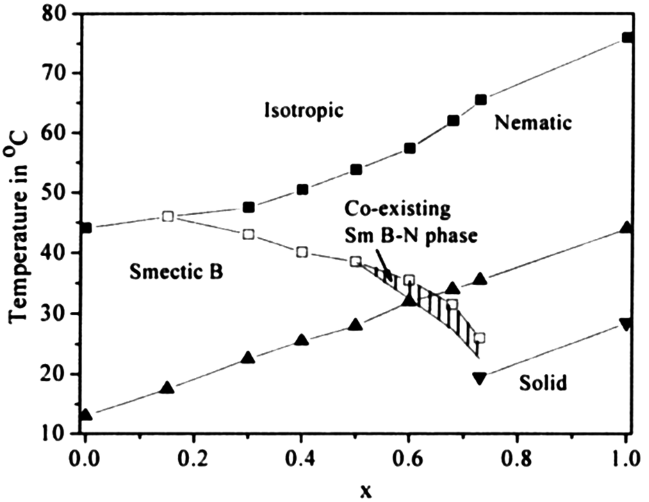

FIGURE 1 Temperature–concentration phase diagram for the binary system of ld(3)CCO_2 and 0d(4)CCO_2. The mole fraction of ld(3)CCO_2 is x. ■ nematic (smectic B)–isotropic transition temperature, □ smectic B–nematic transition temperature, ▲ melting temperature, and ▼ supercooling transition temperature. The shaded region represents the co-existing smectic B–nematic phase.

laboratory, it has been possible to measure the supercooling temperature only for a mixture with $x = 0.73$ and the pure compound ld(3)CCO_2. Texture study of these mixtures showed typical marbled texture in the N phase and a mosaic texture in the SmB phase.

DSC Measurements

Transition entropies ΔS ($J\,mol^{-1}\,K^{-1}$) were obtained from DSC studies (at a heating rate of 1°C/min) for all the mixtures and the pure compounds using a Mettler FP84HT TA Cell.

Density Measurements

The densities of all the binary mixtures were measured with the help of dilatometer of the capillary type. Density measurement of the pure compounds have already been reported [1,2]. Temperature during the experiment was controlled to about ± 0.5°C by a temperature controller. Experimental uncertainty of the density measurement is 0.1%.

Refractive Index Measurements

The ordinary and extraordinary refractive indices (n_o, n_e) for wavelength $\lambda = 5780\,\text{Å}$ of mercury vapor lamp were measured within ± 0.001 by the thin prism method (refracting angle $< 2°$). Details of the experimental technique used have been described by Zeminder *et al.* [6]. From the density and refractive index values, we have calculated the principal polarizabilities $(\alpha_{\|}, \alpha_{\perp})$ using Neugebauer's anisotropic internal field model [7].

RESULTS AND DISCUSSION

From a detailed study of the phase diagram by microscopic observations, it is observed that for mixtures within the concentration range $0.2 < x < 0.8$ (x = molar fraction of ld(3)CCO_2), both SmB and N phases are present. Mixtures with $x < 0.2$ show the SmB phase only and for $x > 0.8$ show the N phase only. For mixtures with molar fractions between $x \approx 0.5$ and $x \approx 0.8$, a two-phase (SmB-N) co-existing region of 2–3°C is observed. The phases could be identified distinctly under the polarizing microscope, and the co-existing phases are quite stable. All the mixtures show large supercooling. The I transition temperature for these mixtures is significantly below the straight line connecting those of the pure compounds, and a fairly deep minimum is observed in the clearing curves for $x \approx 0.4$. The melting temperatures for these mixtures, however, follow the additive rule.

Figure 2 shows the entropy change associated with the SmB-N and N-I phase transition plotted against molar fraction of 1d(3)CCO$_2$. From the figure, it is evident that the entropy change associated with the SmB-N phase transition for these mixtures decreases linearly in the region $x = 0$ to $x = 0.55$ and then falls rapidly at $x = 0.6$. This clearly implies a change in the order of this phase transition from discontinuous to continuous at this value of x (0.6). The N-I entropy change shows a minimum near equimolar concentration.

The variation of ordinary (n_o) and extraordinary (n_e) refractive indices with temperature are shown in Figs. 3a–b for $\lambda = 5780\,\text{Å}$. The ordinary and extraordinary refractive indices are found to be nearly independent of temperature in the SmB phase, except very near to the SmB-N or I transition temperatures for all the mixtures. However, the n_e and n_o values are quite sensitive to temperature in the N phase. In the co-existing SmB-N phase, we have been able

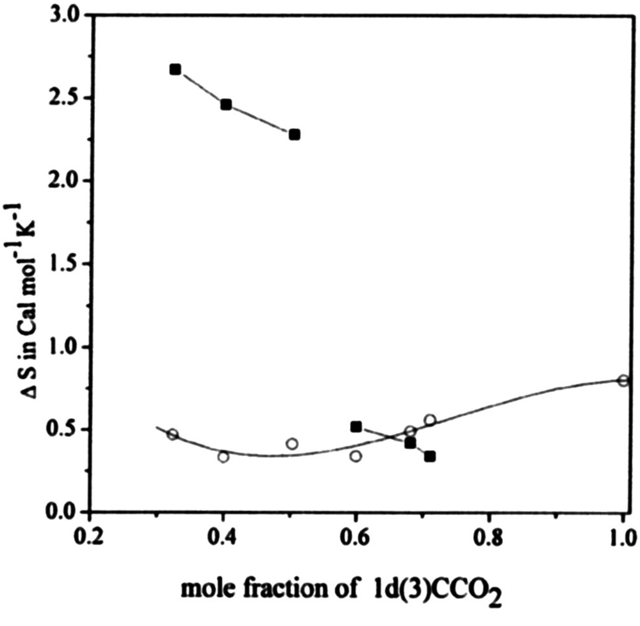

FIGURE 2 Transition entropies (ΔS) as a function of molar fraction of ld(3)CCO$_2$. ■ smectic B/nematic transition, and o nematic/isotropic transition.

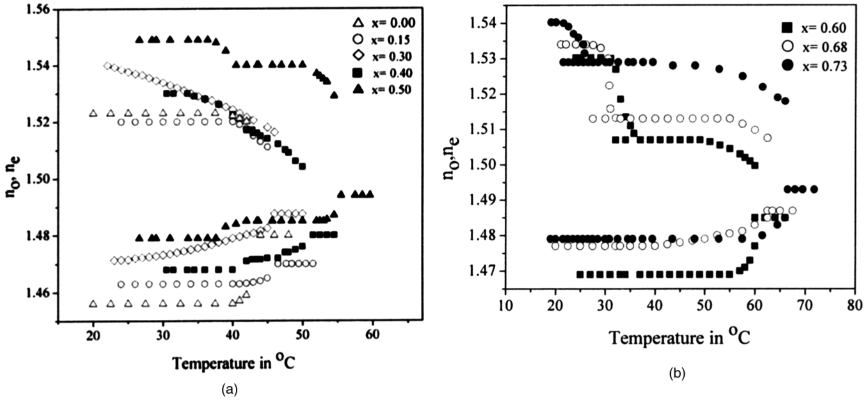

(a) (b)

FIGURE 3 a) Refractive indices as a function of temperature for molar fractions (x) of ld(3)CCO$_2$. Δ (x = 0.0), ○ (x = 0.15), ◇ (x = 0.3), ■ (x = 0.4), and ▲ (x = 0.5); b) Refractive indices (n_o, n_e) as function of temperature for different mixtures. ■ (x = 0.6), ○ (x = 0.68), and ● (x = 0.73).

to simultaneously measure the refractive indices of both the SmB and the N phases. The ordinary refractive indices for SmB and N phases are the same, whereas the extraordinary refractive indices for the

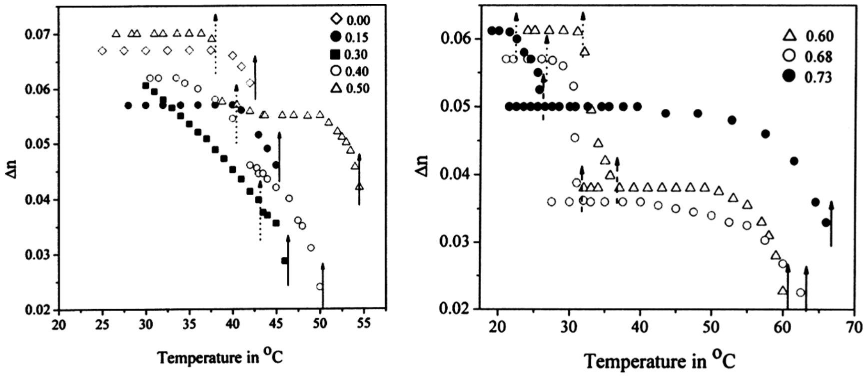

(a) (b)

FIGURE 4 a) Birefringence ($\Delta n = n_e - n_o$) as a function of temperature for different mixtures and a pure compound. ◇ (x = 0.0), ● (x = 0.15), ■ (x = 0.30), ○ (x = 0.4), Δ (x = 0.5), ↑ for nematic to isotropic transition, and ⇡ for smectic B to nematic transition, b) Birefringence ($\Delta n = n_e - n_o$) as a function of temperature for different mixtures: Δ (x = 0.6), ○ (x = 0.68), ● (x = 0.73), ↑ for nematic to isotropic transition, ⇡ for coexisting SmB-N to nematic transition, and ⇡ for SmB to SmB-N coexisting transition.

N phase (n_{en}) and SmB phase (n_{es}) are different. The temperature dependence of n_{es} is large, but n_{en} is more or less independent of temperature.

The optical birefringence Δn ($= n_e - n_0$) values are shown in Figs. 4a–b for these mixtures, which are found to be very low, and are less than 0.1 even in the SmB phase. The temperature dependences of the density values for different mixtures as well as the pure compounds are plotted in Fig. 5. The change of birefringence as well as density values at the SmB-N phase transition seems to be continuous for $x \geq 0.55$, which indicates a weakly first-order or second-order phase transition. On the other hand, mixtures with $x \leq 0.55$ show a sharp discontinuity in the Δn and density values at the SmB-N phase-transition temperature, indicating first-order phase transition, in agreement with the results from DSC measurements. Both the Δn and density values change sharply with temperature within the co-existing SmB-N phase. Also, the temperature dependences of the density values in the SmB phase are much higher for mixtures with $x \leq 0.55$ than in the SmB phase for those mixtures with $x \geq 0.55$. Incidentally, the SmB-N co-existence region is present for mixtures with $x \geq 0.55$. The temperature dependences of the density values show a steep variation within the co-existing phase in comparison to its dependence within its N and SmB neighbors. We

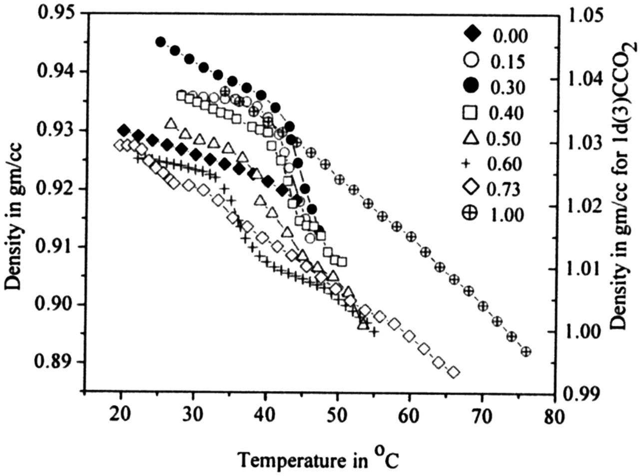

FIGURE 5 Density (ρ) values as a function of temperature for different mixtures and pure compounds. ◆ (x = 0.0), ○ (x = 0.15), ● (x = 0.3), □ (x = 0.4), Δ (x = 0.5), + (x = 0.6), ◇ (x = 0.73), and ⊕ (x = 1.0).

also observe a similar behavior of the Δn values for these mixtures (Figs. 4a–b).

The refractive index and density data have been analyzed to determine the orientational order parameter $\langle P_2 \rangle$. The order parameter and optical properties of the system are connected by the relation

$$\langle P_2 \rangle \Delta\alpha = \alpha_e - \alpha_o$$

where α_e and α_o are the effective polarizabilities for extraordinary and ordinary rays calculated from the measured values of the refractive indices using Neugebauer's approach [7]. $\Delta\alpha = \alpha_{||} - \alpha_{\perp}$, the polarizability anisotropy, can be estimated by applying the well-known Haller's extrapolation procedure [8]. In Fig. 6, we have plotted the concentration dependence of the polarizability anisotropy values for the pure compounds as well as for the different mixtures. We observe a decrease in the values of Δα with increase in the molar fraction of ld(3)CCO$_2$, which shows a broad minimum near x ≈ 0.6, in spite of the arbitrariness involved in the determination of the polarizability anisotropy values using Haller's extrapolation procedure.

The temperature variation of the orientational order parameter $\langle P_2 \rangle$ for the different mixtures is shown in Figs. 7a–b. Similar to the

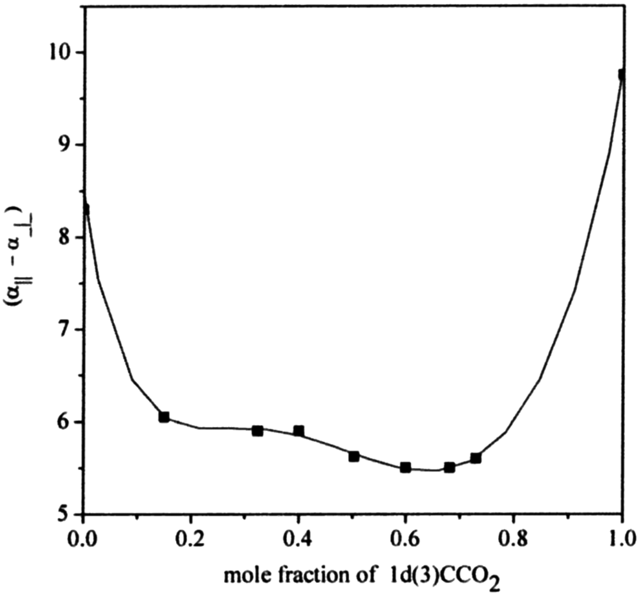

FIGURE 6 Variation of $(\alpha_{||} - \alpha_{\perp})$ against molar fraction of ld(3)CCO$_2$: ■ Neugebauer's method.

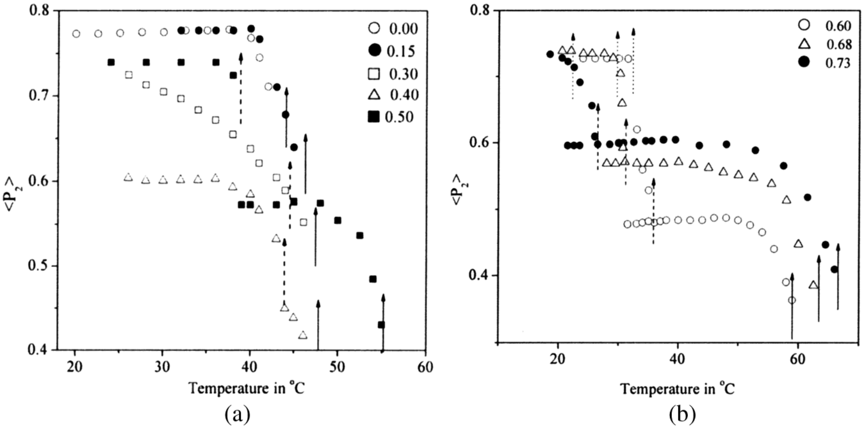

(a) (b)

FIGURE 7 a) Orientational order parameter $\langle P_2 \rangle$ as a function of temperature for molar fractions (x) of ○ ld(3)CCO$_2$ (x = 0.0), ● (x = 0.15), □ (x = 0.3), Δ (x = 0.4), ■ (x = 0.5), ↑ for nematic to isotropic transition, and ⇡ for smectic B to nematic transition, b) Orientational order parameter $\langle P_2 \rangle$ as a function of temperature for different mixtures with molar fractions (x) of ld(3)CCO$_2$. ○ (x = 0.6). Δ (x = 0.68), ● (x = 0.73), ↑ for nematic to isotropic transition, ⇡ for coexisting SmB-N to nematic transition, and ⇡ for SmB to SmB-N coexisting transition.

observed trends in the temperature dependences of the density and birefringence, the $\langle P_2 \rangle$ values also drop sharply at the N-SmB phase transition for mixtures with $x < 0.5$, once again indicating the order of the N-SmB phase transition for these mixtures to be of first order (Fig. 7a). However, the order parameter values change continuously across the N-SmB transition temperatures for mixtures with molar concentration $x > 0.5$ as indicated in Fig. 7b. It is also observed that within the co-existing phase the temperature variation of $\langle P_2 \rangle$ is quite sharp, which corroborates the results of density and refractive index measurements.

Figure 8 shows the variation of $\langle P_2 \rangle$, Δn, and density with molar fraction of ld(3)CCO$_2$ at a temperature $T = T_{NI}(T_{SI}) - 2°C$. The $\langle P_2 \rangle$, Δn, and density values in the N phase show a minimum near $x \approx 0.6$. X-ray diffraction measurements of these mixtures have also been done by us, the details of which are reported in the next part of this work [9]. From such measurements, it has been found that, within the N phase, the intermolecular distance (D) show an enhancement in their magnitudes near $x \approx 0.6$ (Fig. 9), whereas the density and order parameter show a reverse trend. This implies that the packing of the molecules in the N

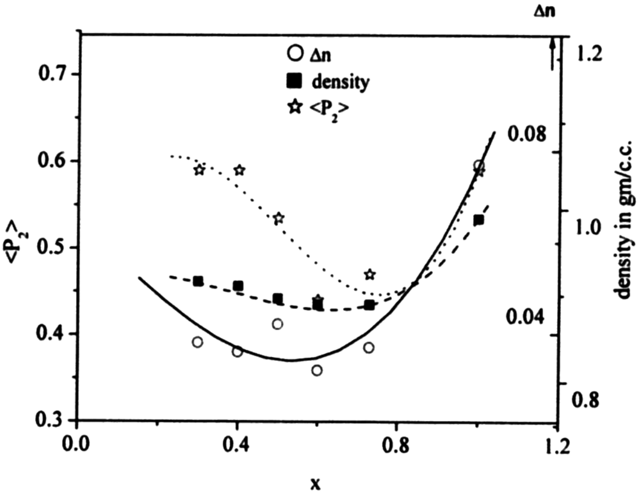

FIGURE 8 Density (ρ), $\langle P_2 \rangle$, and Δn against molar fraction (x) of ld(3)CCO_2 at $T = T_{NI}(T_{SI}) - 2°C$ (■ ρ, ☆ $\langle P_2 \rangle$, and ○ Δn).

phase is poor near $x \approx 0.6$. This variation of D with molar concentration clearly explains why the density and $\langle P_2 \rangle$ values in the N phase decreases near $x \approx 0.6$.

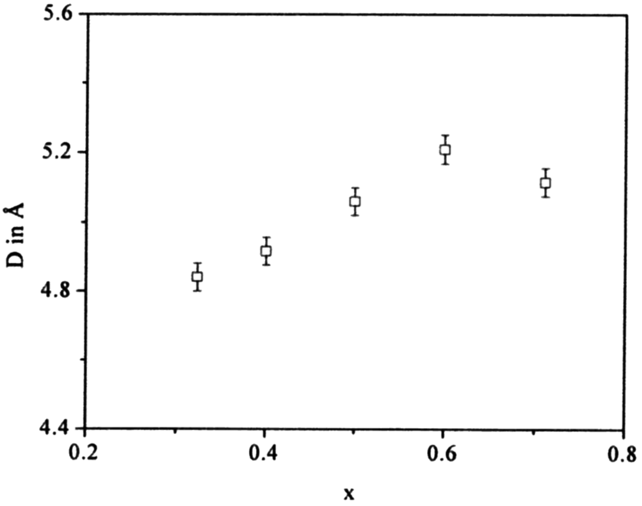

FIGURE 9 Variation of intermolecular distance (D) with molar fraction (x) of ld(3)CCO_2 in the nematic phase.

ACKNOWLEDGMENTS

We are grateful to M/S Hoffmann-La-Roche and Co., Basel, Switzerland, for kindly donating the liquid-crystal line samples used in this work. One of the authors (B. D.) is thankful to the Council of Scientific and Industrial Research, New Delhi, India, for the award of a research associateship.

REFERENCES

[1] Nath, A., Chaudhury, B., & Paul, S. (l995). *Mol. Cryst. Liq. Cryst.*, *265*, 699.
[2] Adhikari, B. & Paul, R. (1996). *Phase Transitions*, *56*, 165.
[3] Nath, A., Gupta, S., Mandal, P., Paul, S., & Schenk, H. (1996). *Liq. Cryst.*, *20*, 765.
[4] Nath, A., Chaudhury, B., & Paul, S. (1995). *Mol. Cryst. Liq. Cryst.*, *265A*, 699.
[5] Schadt, M., Buchecker, R., & Müller, K. (1989). *Liq. Cryst.*, *5*, 293.
[6] Zeminder, A. K., Paul, S., & Paul, R. (1980). *Mol. Cryst. Liq. Cryst.*, *61*, 191.
[7] Neugebauer, H. E. J. (1954). *Can. J. Phys.*, *32*, 1.
[8] Haller, I., Huggins, H. A., Lilienthal, H. R., & McGuire, T. R. (1973). *J. Phys. Chem.*, *77*, 900.
[9] Das, M. K., Roy, P. D., Paul, S., Paul, R., & Das, B. (2006). *Mol. Cryst. Liq. Cryst.*, 457, 55.